IMPACT OF GNSS SIGNAL OUTAGE ON EOPS USING FORWARD KALMAN FILTER AND SMOOTHING ALGORITHM

Arash Jouybari[1*], Mohammad Bagherbandi[1,2], Faramarz Nilfouroushan[1,3]

[1] Faculty of Engineering and Sustainable Development, University of Gävle, Gävle, Sweden - (arhjoi, modbai, faznin)@hig.se
[2] Division of Geodesy and satellite positioning, Royal Institute of Technology (KTH), Stockholm, Sweden
[3] Department of Geodetic Infrastructure, Geodata Division, Lantmäteriet, Gävle, Sweden

Commission II, WG II/1 - Image Orientation

KEY WORDS: Tightly Coupled, Forward Kalman Filter, GNSS/IMU Integration, Smoothing Algorithm, Virtual Reference Station, Exterior Orientation Parameters, Differential GNSS processing.

ABSTRACT:

The global navigation satellite system (GNSS) has been playing the principal role in positioning applications in past decades. Position robustness degrades with a standalone receiver due to GNSS signal outage in mobile mapping systems. The GNSS and inertial measurement unit (IMU) integration is used to solve positioning degradation. This article studies the GNSS/IMU integration processing (i.e., forward Kalman filter (KF) and smoothing algorithm) using a single or a network of nearby GNSS reference stations. In addition, we analyze the impact of simulated GNSS signal outage on exterior orientation parameters (EOPs). The outcomes confirm that the smoothing algorithm works better than the forward KF and improves the accuracy for position and orientation in the case when there is no GNSS signal outage. Also, it improves the position and orientation accuracy by about 95% and 60% when there is a 180 second GNSS signal outage, respectively.

1. INTRODUCTION

For the past few decades, the use of global navigation satellite system (GNSS) technology has drastically expanded in the field of airborne mobile mapping (AMM) systems. The most used navigational solution is integrating GNSS with an inertial measurement unit (IMU) to obtain more accurate results. Both GNSS and IMU systems complement each other and overcome their constraints. In other words, GNSS and IMU provide the position and orientation of the AMM system, respectively, using a GNSS/IMU integration technique.

GNSS/IMU integration sometimes has a significant problem that is linked to GNSS signal outages during the flight mission. The GNSS signal outage can occur because of signal blockage due to e.g., discontinuity in a receiver's phase lock on a satellite's signal such as sharp turn of aircraft, power loss, very low signal to noise ratio, a failure of the receiver software, carrier phase cycle slip because of severe ionospheric conditions (cf. (Skone, 2001); (Feng et al., 2020)). In this case, the IMU supplies a navigation solution during a GNSS signal outage. But IMUs can only provide a short-time high-accuracy navigation that decreases over time (Jouybari et al., 2017); (Jouybari et al., 2019); (Nassar et al., 2004); (Jouybari et al., 2021). In addition, the cycle slip detection significantly can affect the final positioning accuracy, which can be done using IMU during GNSS signal outage (Liu et al., 2010).

The differential GNSS/IMU integration processing is performed using a Kalman filter (KF) in either a loosely coupled (LC) or tightly coupled (TC) scheme for precise positioning of mobile mapping system applications (cf. (El-Sheimy et al., 1995); (Chiang et al., 2004); (Nassar and El-Sheimy, 2005)). Figure 1 illustrates the loosely coupled GNSS/IMU integration scheme that is a simpler processing procedure rather than tightly coupled (see Figure 2). Tightly coupled also has an ambiguity fixing capability.

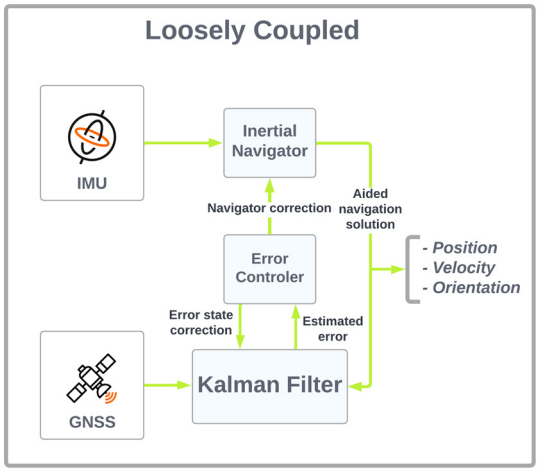

Figure 1. The loosely coupled scheme in GNSS/IMU integration

The KF is accepted as the commonly used optimal estimator in GNSS/IMU integration systems. Also, the KF operates in a prediction mode during GNSS signal outage and relies on stand-alone IMU. KF cannot supply precise exterior orientation parameters (EOPs) (position and orientation of the camera center) due to the time-dependent accumulative errors of IMU. Therefore, a post-processing two-way (forward and backward direction processing) smoothing algorithm should be applied to obtain more accurate EOPs.

*Corresponding author

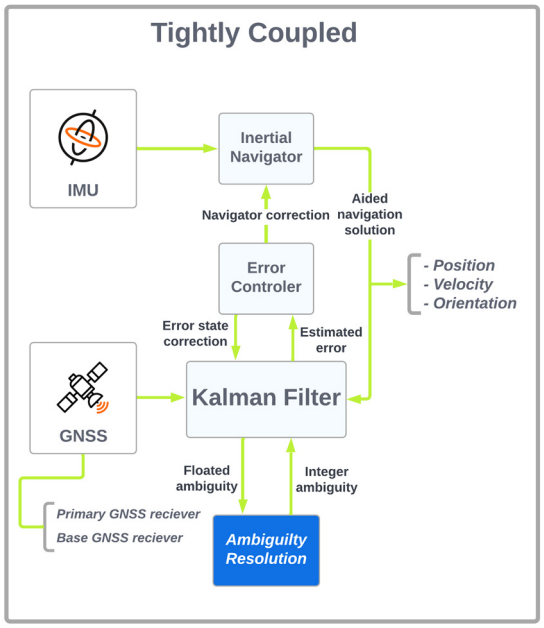

Figure 2. The tightly coupled scheme in GNSS/IMU integration

Both KF and smoothing algorithms establish based on minimum variance estimation in which both observations and parameters act under Gaussian distribution. Also, a nonlinear system should be linearized with Tailor series because both KF and smoothing algorithms are established using a linear system (Dougherty, 2009); (Vaclavovic and Dousa, 2015). However, smoothing algorithms have been efficiently used in post-processing GNSS/IMU integrations to overcome the drawbacks of filtering procedures. The forward and backward direction processing was used to find the best state estimate for each epoch of time (Chiang et al., 2012). Rauch et al. (1965) developed a famous recursive algorithm called Rauch-Tung-Strieble (RTS) smoother. RTS utilizes standard KF and maximum likelihood estimation in the forward and backward direction, respectively. Brayson and Frazier M. (1963), also utilized maximum likelihood and applied it in their smoother algorithm but in a continuous system. However, RTS applies only to discrete systems. Besides, RTS implementation is straightforward and with high reliability. (Zhang and Li, 1996) devised a fixed interval smoothing algorithm based on singular value decomposition (SVD). The idea was to combine a forward direction SVD-based square-root KF with the RTS backward direction recursive smoother using the SVD as a main computational tool. Also, (Park and Kailath, 1996) used a new square-root form for three well-known smoothing formulas (i.e. RTS (Rauch et al., 1965), Desai-Weinert-Yusypchuk (Desai et al., 1981), Mayne-Fraser (Mayne, 1966)).

Liu et al. (2010) developed a two-filter smoother (TFS) and applied it in GPS/IMU integration for land-vehicle navigation applications. The estimations accuracy and computational time of TFS and RTS were close. Furthermore, position error improvement using the smoother algorithm enhanced from %35 to %95 with comparing forward KF, depending on the length of GPS signal outage. Cao and Mao (2008) replaced unscented KF with square-root KF in a forward-pass filter and two smoothers (i.e., fixed-interval and fixed-lag smoother) used in backward-pass smoothing. The final result was not satisfying because they used only code data of GPS and not precise carrier phase data. Chiang et al. (2009) merged artificial neural networks and RTS smoothing for better GNSS/IMU integration. The research showed that the computational time of the aforementioned algorithm was significantly more due to the training process. But it improved approximately 70% compared with RTS. Overall, the estimation accuracy of smoothing is better than that of filtering.

In this study, we compare different GNSS/IMU integrations for EOPs computation. In other words, we evaluate different configurations of GNSS base stations (i.e., single and network GNSS reference stations) employing forward KF and smooth algorithms. In addition, we assess the GNSS signal outage problem, which can be occurred during data collection in the AMM system.

2. MAIN BODY

2.1 Materials and method

The airborne data set (aerial images, GNSS, and IMU data) was captured in May 2017 in Sweden's Halland region. The dual-frequency SWEPOS base station dataset with a 15-sec data rate is the second data set that is processed beside the airborne trajectory. The numbers of SWEPOS base stations were seven base stations. Figure 3 shows the SWEPOS base station's location (in the middle of the network) and the AMM trajectories in which the longest 3D distance to the closest GNSS base station is less than 40 km in the study area.

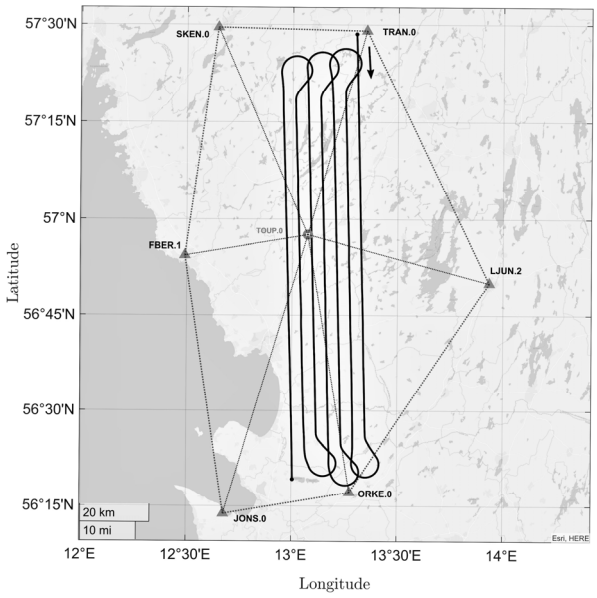

Figure 3. The aircraft trajectory and a configuration of the SWEPOS GNSS reference station

Two post-processing modes (loosely and tightly coupled) integrate the IMU and GNSS observables and a tightly coupled integration algorithm is used in this study. The tightly coupled fulfilled with single and network reference stations. Tightly coupled with a single or network reference station calculates EOPs using forward Kalman filter (KF) and a common post-processing smoothing method. Figure 4 gives a better understanding of the procedure of the process. In which tightly coupled GNSS/IMU integration is done with a single reference station and a network of reference stations.

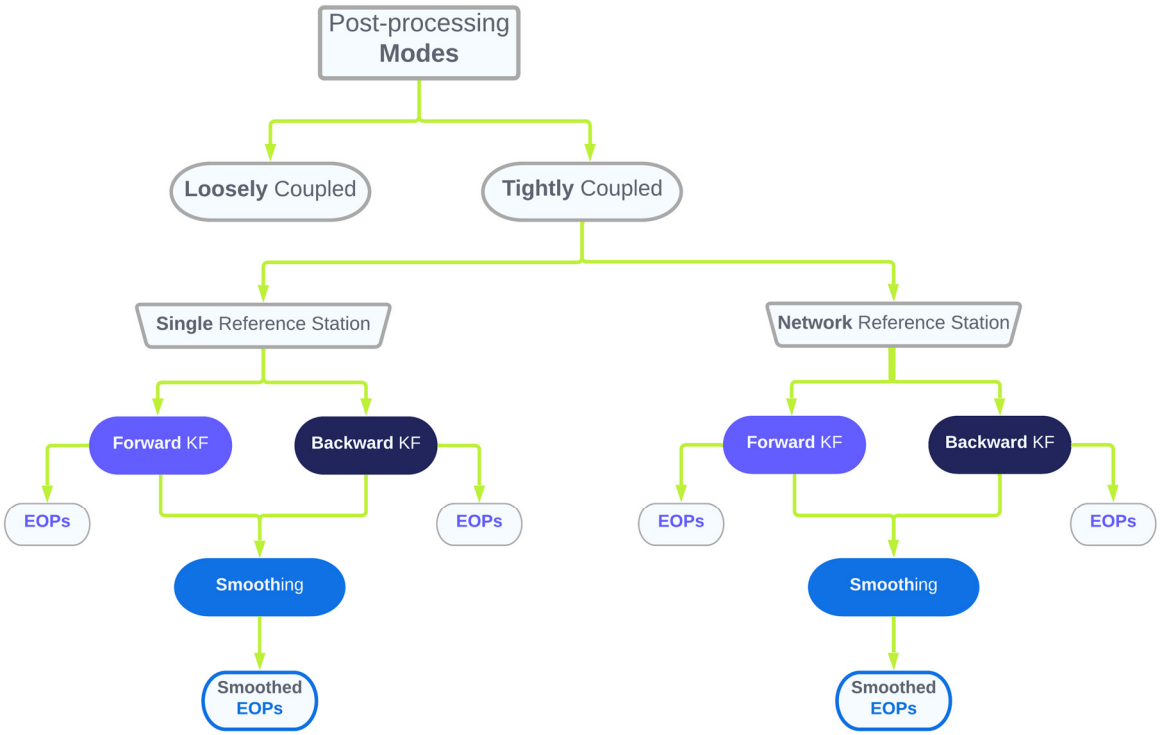

Figure 4. A schematic view of the post-processing sequences used for GNSS/IMU integration processing

2.2 Results

Before evaluating the GNSS signal outage with different durations, it is crucial to analyze which integration method gives the best outcome assuming without the GNSS signal outage. The EOPs are calculated with the following integration methods: single reference station with forward KF, network reference station with forward KF, single reference station with smooth processing, and network reference station with smooth processing.

2.2.1 Single and network solution comparison: The EOPs uncertainties were calculated for the position (north, east, height) and orientation (roll, pitch, heading) using the above-mentioned processing methods. The positional components (north, east, and height) component uncertainties obtained by the forward KF method follow a forward-wise error decrease. At the same time, the smooth processing is more uniform and consistently are more accurate than the forward KF processing in position (c.f. (Cao and Mao, 2008); (Liu et al., 2010); (Zhang et al., 2020). In addition, processing with single and network reference stations is almost the same, but the network solutions are more accurate than single reference station processing. Based on Table 1, the mean values of position uncertainties using smooth processing for single and network solutions are close to each other and better than the solutions for the forward KF processing. Similarly, the mean values of orientation uncertainties using smooth processing (for single and network solutions) are the same and better than the forward KF processing. Roll and pitch uncertainties are approximately 2.5 times better than heading uncertainties in all processing modes.

EOPs	Processing Modes	Units	Max	Mean	Min	STD
North	SF	mm	63	52	32	5.2
	NF		60	51	29	5.2
	SS		45	43	27	3
	NS		44	42	24	3.2
East	SF	mm	59	39	28	9.1
	NF		57	38	26	8.7
	SS		45	27	25	3.9
	NS		43	26	24	3.7
Height	SF	mm	78	48	38	10
	NF		75	46	37	9.9
	SS		32	27	25	1.3
	NS		30	26	24	1.3
Roll	SF	arcmin	3.6	0.65	0.27	0.78
	NF		3.6	0.65	0.27	0.79
	SS		0.41	0.25	0.2	0.048
	NS		0.41	0.25	0.2	0.048
Pitch	SF	arcmin	3	0.64	0.27	0.74
	NF		3	0.63	0.27	0.74
	SS		0.42	0.25	0.2	0.049
	NS		0.42	0.25	0.2	0.049
Heading	SF	arcmin	11	1.7	0.62	1.6
	NF		11	1.7	0.61	1.6
	SS		1.5	0.66	0.41	0.24
	NS		1.5	0.66	0.4	0.24

Table 1. Statistical information of EOPs uncertainties in Single-Forward (SF), Network-Forward (NF), Single-Smooth (SS), and Network-Smooth (NS) processing methods.

2.2.2 Smooth and forward KF processing comparison: The network solutions, using forward KF and smooth processing methods, are selected for evaluating the impact of different GNSS signal outage durations on EOPs accuracy according to the obtained results. In this study, simulated GNSS signal outages consist of 30, 60, 120, 180 seconds considered in the GNSS/IMU integration processing. EOPs (north, east, height, roll, pitch, and heading) uncertainties using forward KF and Smoothing method have been calculated. The obtained results of the processing are illustrated as the uncertainty plots during GNSS signal outage in the following plots.

Figures 5 and 7 illustrate the height uncertainty during GNSS signal outage for forward KF and smooth methods. Figures 6 and 8 show the roll uncertainty during GNSS signal outage for forward KF and smooth methods, respectively. The height uncertainties (Figure 5), in the forward KF processing, in the worst case (i.e., 180 sec GNSS signal outage) are almost 23 and 21 times worse than smooth processing (Figure 7), respectively. However, the roll and heading uncertainties, using the forward KF processing (Figures 6 and 9), in the worst case (180 seconds GNSS signal outage) are almost 2.5 times worse than smooth processing (Figures 8 and 10).

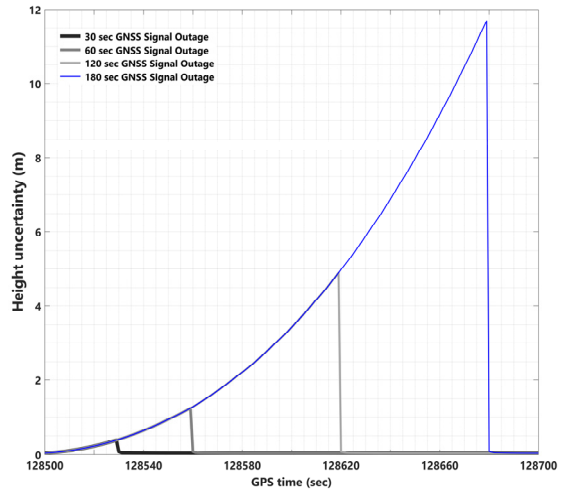

Figure 5. Height uncertainties using forward KF processing and assuming different GNSS outage durations.

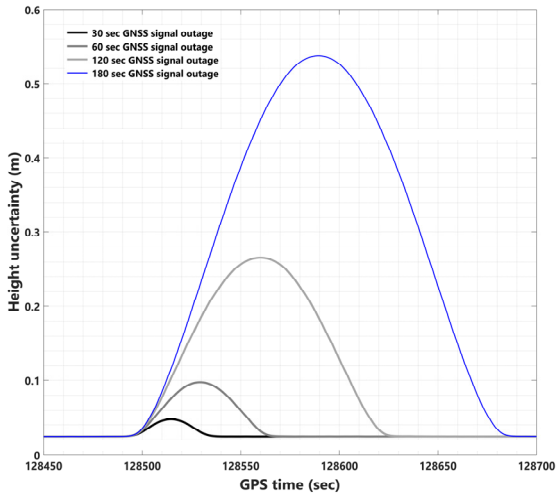

Figure 7. Height uncertainties using smooth processing and assuming different GNSS signal outages.

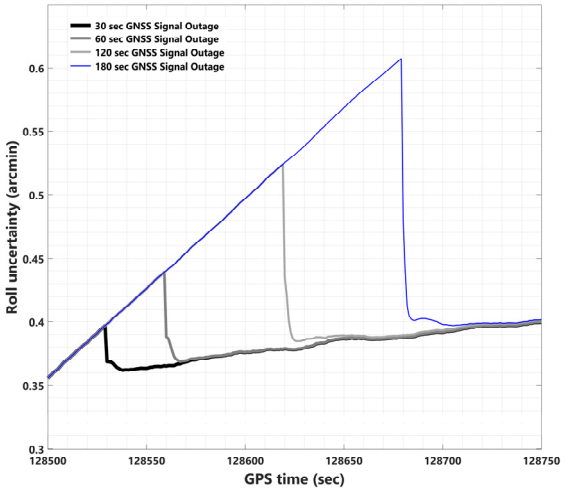

Figure 6. Uncertainties of the roll using forward KF processing and assuming different GNSS signal outages.

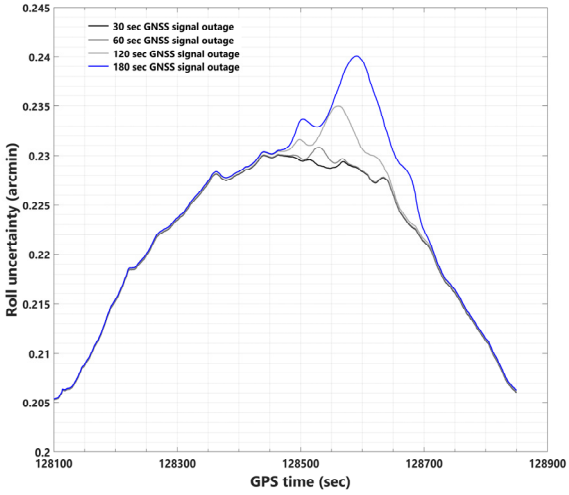

Figure 8. Uncertainties of the roll angle using smooth processing and assuming different GNSS signal outages.

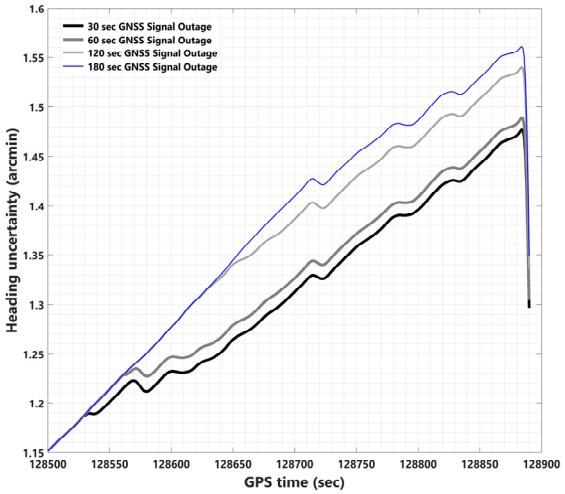

Figure 9. Uncertainties of heading using forward KF processing and assuming different GNSS outage durations.

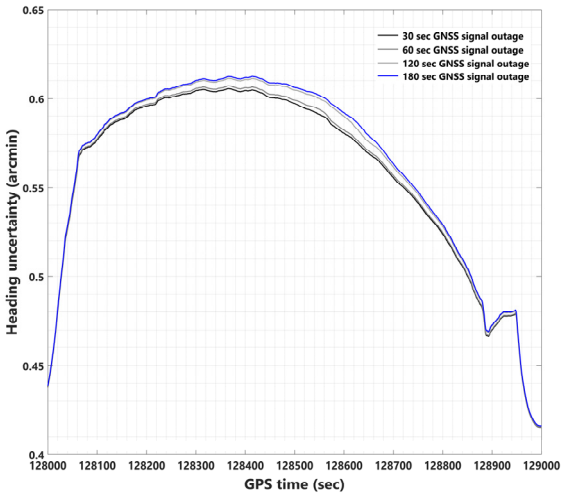

Figure 10. Uncertainties of heading using smooth processing and assuming different GNSS signal outages.

3. Conclusions

In summary, this study argued the implementation of forward KF and smoothing algorithm in GNSS/IMU integration using a single and a network of GNSS reference stations. In addition, the GNSS signal outage has been simulated in EOPs calculation to examine the effect of the GNSS signal outage. Our study shows that the smoothing algorithm gives more robust EOPs using a network of GNSS references stations distributed around the project area with a proper configuration. Besides, the duration of GNSS signal outage directly influences the final EOPs accuracy, in which by increasing the duration, the errors will increase. However, their effect on the position (north, east, height) is more than on orientation (roll, pitch, heading).

4. Acknowledgements

The authors acknowledge the support of Lantmäteriet (the Swedish mapping, cadastral and land registration authority) for providing the Photogrammetric dataset, analyzing software, and sharing their pearls of wisdom with us during this research.

5. References

Brayson, A.E., Frazier M., 1963. Smoothing for Linear and Nonlinear Dynamics Systems. Proc. Optim. Syst. Synth. Conf. 353–364.

Cao, Y., Mao, X., 2008. Improved filtering-smoothing algorithm for GPS positioning, in: IEEE Conference on Intelligent Transportation Systems, Proceedings, ITSC. pp. 857–861. https://doi.org/10.1109/ITSC.2008.4732683

Chiang, K.-W., Chang, H.-W., Li, C.-Y., Huang, Y.-W., 2009. An Artificial Neural Network Embedded Position and Orientation Determination Algorithm for Low Cost MEMS INS/GPS Integrated Sensors. Sensors 9, 2586–2610. https://doi.org/10.3390/s90402586

Chiang, K.W., Duong, T.T., Liao, J.K., Lai, Y.C., Chang, C.C., Cai, J.M., Huang, S.C., 2012. On-line smoothing for an Integrated Navigation System with low-cost MEMS inertial sensors. Sensors (Switzerland) 12, 17372–17389. https://doi.org/10.3390/s121217372

Chiang, K.W., Hou, H., Niu, X., El-Sheimy, N., 2004. Improving the positioning accuracy of DGPS/MEMS IMU integrated systems utilizing cascade de-noising algorithm, in: Proceedings of the 17th International Technical Meeting of the Satellite Division of the Institute of Navigation, ION GNSS 2004. pp. 809–818.

Desai, U.B., Weinert, H.L., Yusypchuk, G.J., 1981. DISCRETE-TIME COMPLEMENTARY MODELS AND SMOOTHING ALGORITHMS: THE CORRELATED NOISE CASE., in: Proceedings of the IEEE Conference on Decision and Control. IEEE, pp. 1048–1053. https://doi.org/10.1109/cdc.1981.269378

Dougherty, E.R., 2009. Random Processes for Image and Signal Processing, Random Processes for Image and Signal Processing. SPIE Optical Engineering Press. https://doi.org/10.1117/3.268105

El-Sheimy, N., Schwarz, K.P., Wei, M., Lavigne, M., 1995. VISAT: a mobile city survey system of high accuracy, in: Proceedings of ION GPS. pp. 1307–1315.

Feng, W., Zhao, Y., Zhou, L., Huang, D., Hassan, A., 2020. Fast cycle slip determination for high-rate multi-GNSS RTK using modified geometry-free phase combination. GPS Solut. 24, 1–11. https://doi.org/10.1007/s10291-020-0956-6

Jouybari, A., Amiri, H., Ardalan, A.A., Zahraee, N.K., 2019. Methods comparison for attitude determination of a lightweight buoy by raw data of IMU. Meas. J. Int. Meas. Confed. 135, 348–354.

https://doi.org/10.1016/j.measurement.2018.11.061
Jouybari, A., Ardalan, A.A., Rezvani, M.H., 2017. Experimental comparison between Mahoney and Complementary sensor fusion algorithm for attitude determination by raw sensor data of Xsens IMU on buoy. Int. Arch. Photogramm. Remote Sens. Spat. Inf. Sci. - ISPRS Arch. 42, 497–502. https://doi.org/10.5194/ISPRS-ARCHIVES-XLII-4-W4-497-2017
Jouybari, A., Bagherbandi, M., Nilfouroushan, F., 2021. Comparison of the strip- and block-wise aerial triangulation using different exterior orientation parameters weights. J. Spat. Sci. https://doi.org/10.1080/14498596.2020.1871086
Liu, H., Nassar, S., El-Sheimy, N., 2010. Two-filter smoothing for accurate INS/GPS land-vehicle navigation in urban centers. IEEE Trans. Veh. Technol. 59, 4256–4267. https://doi.org/10.1109/TVT.2010.2070850
Mayne, D.Q., 1966. A solution of the smoothing problem for linear dynamic systems. Automatica 4, 73–92. https://doi.org/10.1016/0005-1098(66)90019-7
Nassar, S., El-Sheimy, N., 2005. Wavelet analysis for improving INS and INS/DGPS navigation accuracy. J. Navig. 58, 119–134. https://doi.org/10.1017/S0373463304003005
Nassar, S., Noureldin, A., El-Sheimy, N., 2004. Improving positioning accuracy during kinematic DGPS outage periods using SINS/DGPS integration and SINS data de-noising. Surv. Rev. 37, 426–438. https://doi.org/10.1179/sre.2004.37.292.426
Park, P.G., Kailath, T., 1996. New square-root smoothing algorithms. IEEE Trans. Automat. Contr. 41, 727–732. https://doi.org/10.1109/9.489212
Rauch, H.E., Tung, F., Striebel, C.T., 1965. Maximum likelihood estimates of linear dynamic systems. AIAA J. 3, 1445–1450. https://doi.org/10.2514/3.3166
Skone, S.H., 2001. The impact of magnetic storms on GPS receiver performance. J. Geod. 75, 457–468. https://doi.org/10.1007/s001900100198
Vaclavovic, P., Dousa, J., 2015. Backward smoothing for precise GNSS applications. Adv. Sp. Res. 56, 1627–1634. https://doi.org/10.1016/j.asr.2015.07.020
Zhang, X., Zhang, Y., Zhu, F., 2020. A method of improving ambiguity fixing rate for post-processing kinematic GNSS data. Satell. Navig. 2020 11 1, 1–13. https://doi.org/10.1186/S43020-020-00022-Y
Zhang, Y., Li, X.R., 1996. Fixed-interval smoothing algorithm based on singular value decomposition. IEEE Conf. Control Appl. - Proc. 916–921. https://doi.org/10.1109/CCA.1996.559012